

Low Pressure Carburizing Cycle Determination for High Alloy Steels

Zhichao Li, B. Lynn Ferguson, Tianyu Yu, and Justin Sims

DANTE Solutions, Inc.
7261 Engle Road, Suite 105
Cleveland, OH 44130
USA

(440) 234-8477 Charlie.Li@dante-solutions.com

Abstract

High hardenability steels with high alloy content typically contain strong carbide forming elements such as chromium and molybdenum. During carburization, alloys with high amounts of strong carbide formers may form stable carbides on or near the surface during carburization that can effectively block carbon diffusion and retard the carburization process. This is especially true for low pressure carburization where the surface carbon content can rise quickly as the carbon source gas dissociates on the hot part surface. To get carbon penetration into the part and achieve the desired case depth, the low pressure carburization process must consist of a series of boost and diffusion steps in order to control the surface carbon content and the amount of carbides that are present. At issue is how to determine an acceptable carburization schedule in terms of boost and diffusion step times. This presentation will discuss a methodology used to develop a proper low pressure carburizing schedule for these high alloy steels. This methodology involves experiments to determine carbon diffusion rates, carbide formation kinetics, and carbide dissolution kinetics, and computer simulation of the process.

Introduction

The power transmission gear industry, especially aerospace applications, has been pushed to increase power density of the transmission for improved acceleration, load capacity, and extended life. In addition, the safety issue of performing for extended time under poor lubrication conditions where gear temperatures are high and resistance to softening is required are especially important for military applications. Consequently, the gear industry has turned to carburizing grades of ultrahigh strength steels. These steels have high alloy content, with reliance on strong carbide forming elements such as chromium and molybdenum, such that they exhibit secondary hardening during tempering at relatively high temperatures, i.e. $\sim 500^\circ\text{C}$. Examples of these steels include alloys such as Pyrowear 53, Pyrowear 675, Ferrium C64, and CSS-422L, and their nominal chemistries are given in Table 1. The high amounts of the strong carbide forming elements affect the carburization process.

Comparing Gas Carburizing and Low Pressure Carburizing

Since both conventional gas carburizing and low pressure carburizing diffuse carbon into the target components, how are they different? The answer focuses on what happens at the surface of the part.

Gas Carburization: Figure 1 is a graphical representation of what happens during gas carburization.[1] A carbon potential, C_p , exists within the furnace chamber due to the gas composition, which incidentally is at one bar pressure or just slightly over one bar as a positive pressure is maintained in the furnace. The base carbon of the steel part, C_0 , is lower than the gas carbon potential, so carbon is deposited on the part surface, where it then diffuses into the part. As the surface reaction continues, a boundary layer, β , exists as the neighboring gas carbon potential is reduced. D_c is the diffusion coefficient of carbon in the steel. With time, the surface carbon level, C_s , increases, and the carbon level within the steel increases. The process takes time, typically six or more hours, depending on the desired depth of case, process temperature, etc. A key is that the atmosphere carbon potential does not exceed the maximum solubility of carbon in the austenitized steel.

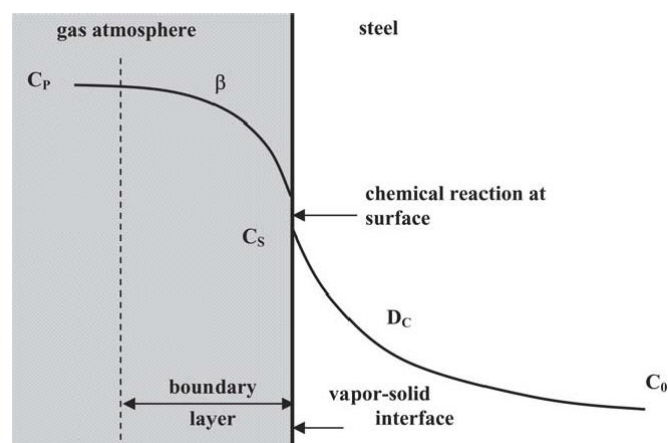


Figure 1: Graphic representation for gas carburization.[1]

This description is simplistic, but the key is maintaining the surface carbon level below the saturation level so that carbides do not form. The furnace response is slow, so a carbon

potential that is too high will result in massive carbides in the final product that will degrade performance.

From Table 1, steel alloys that are gas carburized have levels of strong carbide formers, other than iron, that total less than 1 weight percent. With typical carburizing temperatures of 900 C to 950 C (1650 F to 1750F), gas atmosphere carbon potentials typically range from 0.8% to 1.3%, with the lower values being more common. As the alloy content increases, as for 9310 steel, the carbon potential may be adjusted from high at the beginning of the process, to a lower value for the remainder of the process to help guard against carbide formation. Steps like preoxidation may be added to the process to further reduce the potential for alloy carbide formation and allow greater carbon diffusion into the base metal.

Table 1: Carburizing Steels Showing Base Carbon Level and Amount of Strong Carbide Forming Elements.

	Alloy	%C	%Cr	%Mo	%V	Other
Typical Carburizing Steel Grades	AISI 1020	0.2	-	-	-	
	AISI 4120	0.2	0.5	0.17	-	
	AISI 4320	0.2	0.5	0.25	-	
	AISI 5120	0.2	0.8	-	-	
	AISI 8620	0.2	0.5	0.2	-	
Historic Aerospace Gear Steel	AISI 9310	0.1	1.2	0.12	-	
High Strength Carburizing Steels	Pyrowear 53	0.1	1.0	3.0	2.0	Mn, Si, Cu
	Pyrowear 675	0.07	13.0	1.8	0.6	Co
	Ferrium C64	0.11	3.5	1.75	-	Co, W
	CSS-422L	0.12	14.0	4.75	0.6	Co
	M50NiL	0.12	4.5	4.0	1.2	Ni
	Vasco X2-M	0.15	5.0	1.4	0.5	Mn, Si

The equations used to predict the development of the carburized case in terms of time, temperature, and atmosphere carbon potential are quite simple, as differences between boundary diffusion and bulk diffusion are not considered and carbon potential is held below austenite saturation level. Because the gas carburizing times are long, i.e. several hours, the full carbon potential is immediately applied to the surface of the part. The well known Harris equation can be used to calculate total case depth for gas carburization[2]:

$$\text{Case depth} = f * \sqrt{t} \quad (1)$$

where t is time in hours and f is a temperature dependent factor that is related to diffusion. Notice that there is no relation to different modes of diffusion (boundary or bulk), and there is no provision for alloy effects. Yet, this equation works fairly well for the commonly carburized grades of carbon and low alloy steel.

Many equations for carbon diffusion coefficient in iron and low alloy steels have been published. Three equations for diffusion coefficient D expressed as cm²/s are:

$$D(T,C)=0.47*\exp[-1.6*C]*\exp[-(37000-6600*C)/R/T] \quad (2)$$

$$D(T,C)=(0.04+0.08*C)*\exp[-31350/R/T] \quad (3)$$

$$D(T,M,C)=(0.146-0.036*C*(1-1.075*Cr)+\sum k_1*M)*\exp[-(144.3-15.0*C+0.37*C^2+\sum k_2*M)/R/T] \quad (4)$$

where T is temperature, °K,
 C is weight percentage of carbon,
 k₁ and k₂ are multiplying factors for specific elements,
 M is weight percentage of Mn, Si, Ni, Cr, Mo, or Al,
 R is the universal gas constant, 1.986 cal/mol/°K, and
 R_{kj} is the gas constant expressed as kJ/mol/°K.

These equations are valid within particular chemistry ranges, as discussed in references [3] for eq.(2), [4] for eq.(3), and [5] for eq.(4). A graphical comparison of these equations is shown in Figure 2, where it is obvious that diffusion coefficient increases markedly with temperature, and also with carbon content. What is not as clear is the effect that alloying elements, especially chromium, have on carbon diffusion.

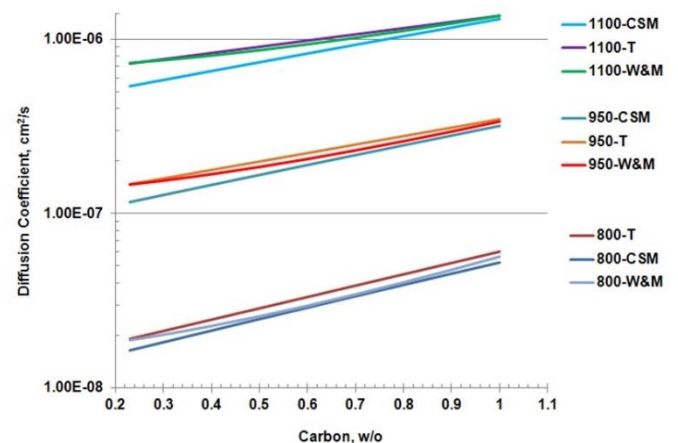
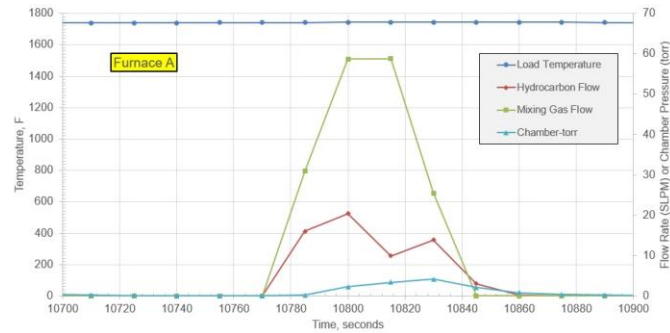


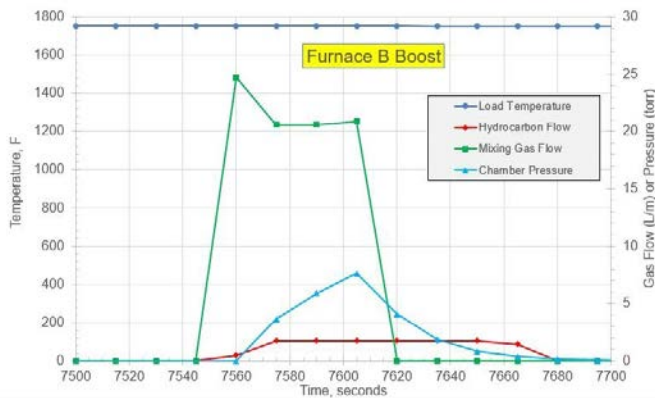
Figure 2: Calculated diffusion coefficient as a function of carbon percentage at three temperatures, 800 C, 950 C and 1100 C. 'T' is for eq.(2), 'W&M' is for eq.(3), and 'CSM' is for eq. (4).

Low Pressure Carburization: Low pressure carburization, as the name implies, is conducted in vacuum furnaces at pressures of about 0.1 to 1 torr. During heating to the carburizing temperature, a nonreactive gas such as nitrogen may be added to provide convection to speed heating through the lower temperatures where radiation is less effective. As the temperature increases, the parts must be protected from surface oxidation, so the vacuum must be below 0.1 to 0.3 torr. A partial pressure of a “surface cleaning” gas such as hydrogen may be added during this stage to make the steel alloy more receptive to carbon absorption. Once the parts have been heated to the desired temperature, carburization commences as a series of boost and diffuse steps. For reasons discussed below, the boost steps are short, typically less than two minutes, and the diffuse steps may be initially similar time, but become progressively longer as the case develops.

Acetylene (C_2H_2) is commonly used as the carbon source gas. During a boost step, the hydrocarbon gas may be blended with another gas such as nitrogen or hydrogen to assist mixing of the hydrocarbon gas in the vacuum chamber. The boost pulse time, gas flows and chamber pressure for two similar furnaces but of different sizes are shown in Figure 3 a and b. Due to size differences, the effective gas flows and chamber pressure are different for a boost step with the same common aim.



(a) Boost step for furnace A.



(b) Boost step for furnace B.

Figure 3. Comparison of boost steps for furnaces of similar design but different sizes.

Carbon Solubility and Alloy Chemistry: The equilibrium phase diagram changes as the chromium content is increased, with the austenite field becoming smaller.[6] A section of the Fe-C phase diagram is shown in Figure 4 and for comparison, an isopleth for the Fe-C-Cr ternary phase diagram for 5% Cr is shown in Figure 5. In Figure 4, austenite saturation with carbon does not occur at carburizing temperatures until the carbon level exceeds about 1.5%C. At higher temperatures, even more carbon can be held in solution in austenite. Figure 5 for 5%Cr shows that the austenite phase field is smaller at this Cr level, and the eutectoid composition is also decreased. The reduced size and shift of the austenite zone means that austenite will saturate at lower carbon levels in steels with higher chromium content than in steels with lower chromium content, and alloy carbides can more readily form. For steels with yet high chromium content, such as P675, the austenite field is indeed small and the potential for alloy carbide formation is high. The possibility of forming many types of carbides becomes widely spread over the elevated temperature range. While these diagrams are for equilibrium and carburizing is a transient process, the diagrams show the

Iron-Carbon Phase Diagram

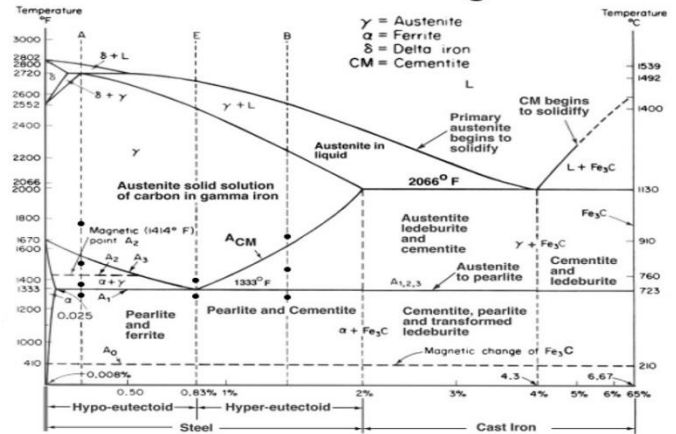


Figure 4: Portion of Fe-C equilibrium phase diagram.[6]

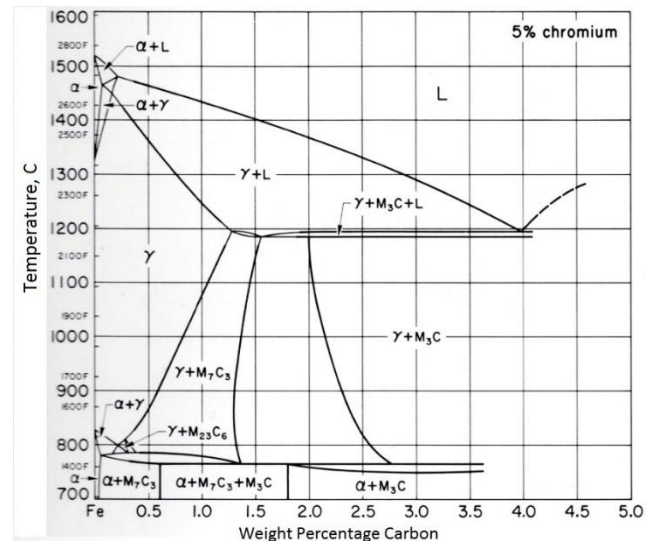


Figure 5: Isopleth from Fe-Cr-C ternary phase diagram for 5% Cr.[6]

increased difficulty of avoiding carbide formation during carburization as carbon is added to steels with higher chromium content. Reference [7] reports that chromium effectively decreases the diffusion of carbon in steel, and this is largely a result of the strong affinity of chromium for carbon. Table 1 shows that austenite stabilizers such as Ni and/or Co are often used in high Cr and Mo steels to counteract the shrinkage of the austenite phase field.

For high strength steels, the carburization must be tightly controlled because the austenite phase field exists under tighter bounds of temperature and carbon level. The simple equation mentioned to calculate case depth no longer holds, as the possible formation of carbides greatly affects carbon diffusion, with carbide formation at part surfaces effectively blocking carbon diffusion.[8] The carburizing process must be designed with carbide formation in mind. While this is also true for gas carburizing, it is especially critical for low pressure carburizing.

The carbon source in low pressure carburizing is a gas or mix of gases that dissociate at the hot part surface to deposit carbon. The carbon source gas dissociates directly on the hot part surfaces, instantly providing carbon that is available to diffuse into the steel. Investigators have reported that the gas dissociation first decays the gas molecules to intermediate radical forms that then breakdown to crystalline graphite.[9,10] Hydrogen gas is typically the other product of the dissociation. This pure carbon then diffuses into the steel, with diffusion down grain boundaries superseding diffusion into austenite grains. The concentration of carbon in grain boundaries promotes carbide formation if the gas dissociation reaction is allowed to continue for too long of time or if the partial pressure of carrier gas is too high (too much dissociation). If this boost time is too long for the amount of carbon gas present, surface carbides will form that block carbon diffusion, eventually causing soot and even tar to form. Hence, a short, controlled boost time is typical, meaning the partial pressure of the carbon source gas is reduced to allow time for any minute carbides that formed to dissolve and carbon diffusion to occur to reduce the surface carbon level. Once sufficient diffusion has occurred, the carbon source gas is reintroduced and the boost step scenario repeats. As the process continues, the boost times remain short and the diffuse step times increase since the surface austenite saturates and more time is needed to lower the surface and near-surface carbon levels by diffusion.

Experiments were run using acetylene as the carbon source gas and Ferrum C64 alloy steel to characterize the low pressure carburization process.

Experimental Results and Discussion

Low pressure carburization trials were run using cylinders with a diameter of ~100 mm. LPC tests were conducted following different boost & diffuse schedules and temperatures to generate different carbon and hardness profiles in these cylinders. Using the combinations of profiles and LPC schedules, carbon diffusion was characterized for Ferrum C64. An example trial schedule is shown graphically in Figure 6, and Table 2 lists the times for this series of boost-diffuse steps. By no means is this schedule presented as a preferred schedule.

The procedure for determining the carbon profile was to carefully machine a 0.05 mm layer from the cylinder using a sharp single point lathe cutter while collecting the chips. By sequentially doing this, individual bags of chips with different carbon content were collected. Then, each segregated collection of chips was subjected to LECO testing to determine the carbon content. This is not a fool-proof method, but with care, the results are accurate. A major problem to avoid is overheating of the chips and/or bar during single point turning, which would result in reduced carbon measurement for that sample set. Microhardness measurements were taken on

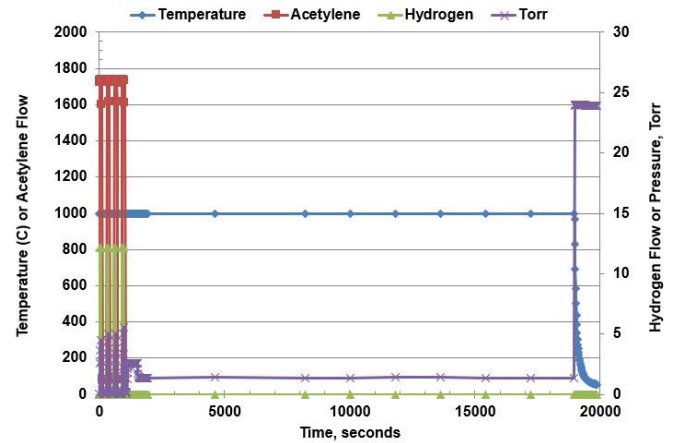


Figure 6: Example LPC schedule followed in one trial run.

Table 2. Trial LPC Schedule.

Step	Step Time, min.	Total Time, min.
Boost 1	1.25	1.25
Diffuse 1	18.0	19.25
Boost 2	0.75	20.0
Diffuse 2	20.0	40.0
Boost 3	0.75	40.75
Diffuse 3	25.0	65.75
Boost 4	0.75	66.50
Diffuse 4	40.0	106.50
Boost 5	0.75	107.25
Diffuse 5	55.0	162.25
Boost 6	0.75	163.0
Final Diffuse	25.0	188.0

metallographically prepared mounted sections for comparison against the carbon weight percentages.

Hardness and carbon profiles determined for four different trial runs are plotted in Figure 7. The relationship between hardness and carbon level for a martensite microstructure for C64 is not published. However, the published data sheet for C64 reports that the Jominy hardness is HRC 43 and that typical core hardness values in carburized parts should be HRC 47 to 50.[10] From Figure 7, the measured microhardness of HRC 45 at a depth of 2 mm should be at the base carbon level of 0.11%. Runs 1-3 were at a carburizing temperature of 1000° C, and run 4 was conducted at a temperature of 940° C. The boost total time was the same for all runs, but the total diffuse time increased from run 1 to run 3, with the diffuse time for run 4 being the same as that of run 2. Observations from Figure 6 are that longer diffuse total time gave deeper penetration of carbon, and that the higher carburization temperature of 1000° C gave a deeper case than the lower 940° C carburizing temperature. These observations are as expected, and they are more easily observed from the hardness data. While the carbon data shows the general trend

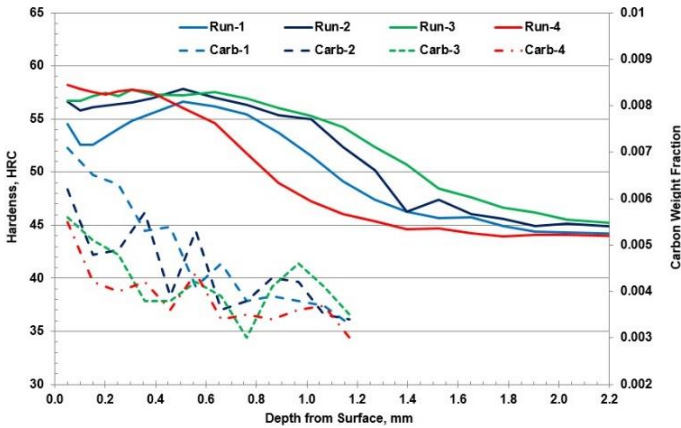


Figure 7: Hardness and carbon profiles measured for a LPC trial.

of being high at the surface and lower with depth from the surface, it has a lot of variation and is more difficult to interpret. Complicating the issue is the possibility of carbide formation and interference with pure diffusion of carbon through the austenite lattice during carburization.

Predicting the development of the final carbon profile must include decisions about carbon saturation of austenite, possible carbide formation and growth, carbide dissolution, and carbon diffusion. Figure 8 shows a framework for such decision making in determining a proper boost – diffuse schedule for an LPC process. Material property data needed to simulate carburization is shown in the block labeled ‘Steel Grade.’ The carburization specification for part will have at a minimum the required case depth (usually hardness at a specified depth), surface hardness and core hardness. These may be specified at particular location(s), and hardness is specified rather than carbon level because it is much easier to measure. For simulation, the part geometry must be known, and for LPC the total surface area to be carburized should be known since the carbon source gas will dissociate on the surfaces of parts and provide the amount of carbon needed to fulfill the case requirement. Once the carrier gas type is specified, the calculations can be made to determine time to saturate austenite at the carburization temperature, i.e. boost step, and the time needed to diffuse carbon away from the surface, i.e. diffuse step. Then the number of boost and diffuse steps can be determined to meet the specified case requirements.

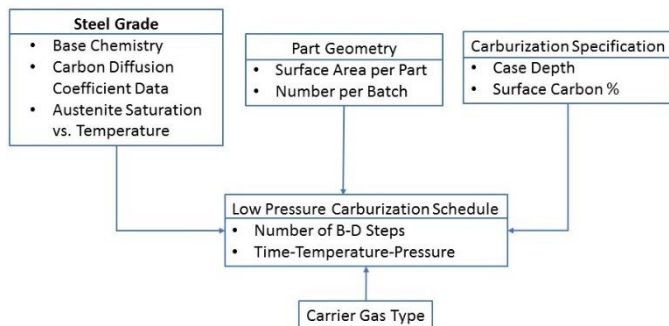


Figure 8: Framework for LPC simulation software.

Figure 9 shows results for a computer simulation that had nine boost and diffuse steps for a LPC run. There are two curves each for two locations, position 501 on the surface and position 492 at a depth of 0.25 mm below the surface. The solid lines are carbon weight fraction predictions, and the dashed lines are normalized carbide size predictions. This boost-diffuse schedule is predicted to produce carbides at the surface that form during the first boost and persist through the entire LPC process. The subsurface location is predicted to form carbides during the last long diffuse step, but these dissolve. From the plot, carbide formation is predicted to occur when the carbon weight fraction hits 0.010. To prevent any carbide formation, the carbon weight fraction should remain below this level **for the steel properties used in this model**. The emphasis on this last phrase is important as the plot in Figure 8 is not for C64, but it is for a competing high strength steel alloy.

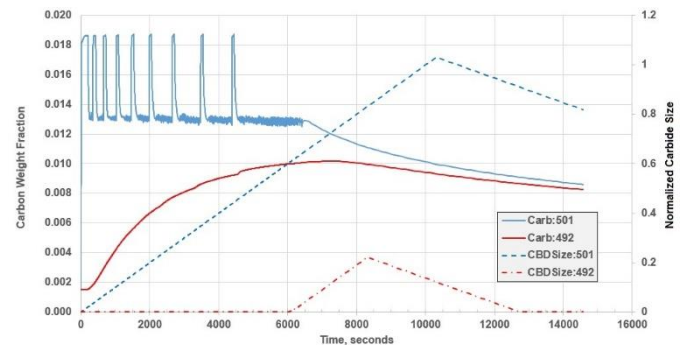


Figure 9: LPC simulation results for a high alloy steel that shows carbide formation and dissolution during a nine step boost – diffuse schedule.

Summary

Modeling carburization of higher alloy content steels, especially alloys containing chromium contents well above 1.0%, requires more than a simplified mass diffusion model. Carbide formation, carbide growth and dissolution all can impact the development of the carburized case. Low pressure carburization has the added complication of rapid carbon build up on the part surface due to direct dissociation of the carbon source gas right on the hot part surface. However, this rapid carbon build up brings with it the ability to more rapidly develop a desired case and also the ability to tailor the shape of the carbon profile. An accurate and comprehensive simulation software gives the heat treater or part designer the ability to take advantage of LPC capabilities while avoiding the possible detriments of excessive surface and grain boundary carbides or surface contamination by soot or tar.

Acknowledgments

The authors wish to acknowledge the support of the US Army ADD for their support of this work and Solar Atmospheres, Inc. for low pressure carburizing the test bars.

References

- [1] Olga Karabelchtchikova, Fundamentals of Mass Transfer in Gas Carburizing, Ph.D. Thesis, Worcester Polytechnic Institute, 2007.
- [2] F.E. Harris, Metals Progress, Vol. 44, pp265-272, 1943.
- [3] G.G. Tibbetts, "Diffusivity of carbon in iron and steels at high temperatures," Journal of Applied Physics, Vol. 51, pp 4813-4816, 1980.
- [4] C. Wells and R. F. Mehl, Trans. AIME, Vol. **140**, 279, 1940.
- [5] .S.J. Lee, D. K. Matlock and C.J. van Tyne, "An Empirical Model for Carbon Diffusion in Austenite Incorporating Element Effects," ISIJ Int., Vol. 51, No. 11, 2011, pp. 1903-1911.
- [6] W.D. Foreng and W.D. Foreng, Jr., "Carbon-Chromium-Iron," Metals Handbook, 8th Edition, vol. 8, ASM, Metals Park, OH, 1973, pp 404.
- [7] L. Nobili, P. Cavallotti and M. Pesetti, "Gas-Carburizing Kinetics of a Low-Alloy Steel," Metallurgical & Materials Transactions A, v41A, February, 2010, pp 460-469.
- [8] L. Zhang and R. Sisson, Jr., "Researchers Perfect Carbon-Concentration Profile Predictions," Industrial Heating, vol. LXXXV No. 3, March 2017, pp 32-35.
- [9] R. Gorockiewicz, A. Adamek, and M. Korecki, "The LPC Process for High-Alloy Steels," Gear Solutions, September, 2008, pp 40-51.
- [10] R. Gorockiewicz, "The kinetics of low-pressure carburizing of alloy steels," Vacuum, Vol. 86, pp 448-451, 2011.